

## Article

# Mineralogical and Geochemical Implications of Weathering Processes Responsible for Soil Generation in Mănăila Alpine Area (Tulgheș 3 Unit—Eastern Carpathians)

Doina Smaranda Sirbu-Radasanu <sup>1,\*</sup>, Ramona Huzum <sup>2,\*</sup> , Delia-Georgeta Dumitraș <sup>3</sup>  and Cristina Oana Stan <sup>1</sup>

<sup>1</sup> Department of Geology, Faculty of Geography and Geology, “Alexandru Ioan Cuza” University of Iași, 20A ‘Carol I’ Blvd., 700505 Iași, Romania

<sup>2</sup> Integrated Center of Environmental Science Studies in the North-Eastern Development Region (CERNESIM), Department of Exact and Natural Sciences, Institute of Interdisciplinary Research, ‘Alexandru Ioan Cuza’ University of Iași, Alexandru Lăpușeanu Street, No. 26, 700057 Iași, Romania

<sup>3</sup> Department INI, Geological Institute of Romania, Caransebeș Street, No. 1, Sect. 1, 012271 Bucharest, Romania

\* Correspondence: doina.sirbu@uaic.ro (D.S.S.-R.); ramona.huzum@gmail.com (R.H.)

**Abstract:** In the Mănăila alpine area, the soil layer developed in situ on top of the sericite-schists, which belong to the Tulgheș 3 metamorphic unit. The aim of the present work was to determine the degree of soil formation using both mineralogical and geochemical exploration methods. XRD, FTIR and SEM-EDS results showed that the soil constituents were dioctahedral 2:1 minerals, quartz, chlorite, Na-feldspar, rutile and ilmenite. Mainly illite and secondarily mixed-layer minerals were considered to be the most likely minerals resulting from the transformation of sericite and chlorite under acidic alpine conditions. Geochemical modeling inferred the dominance of illite and the presence of smectite as a chlorite alteration product. The weathering indices supported the moderate stage of the soil development agreeing with mineralogical observations. Because of the abundance of sericite and quartz in the parent material, the soil formation was retarded, and its present composition is still related to the bedrocks.

**Keywords:** soil mineralogy; soil geochemistry; weathering indices; alpine soil



**Citation:** Sirbu-Radasanu, D.S.; Huzum, R.; Dumitraș, D.-G.; Stan, C.O. Mineralogical and Geochemical Implications of Weathering Processes Responsible for Soil Generation in Mănăila Alpine Area (Tulgheș 3 Unit—Eastern Carpathians). *Minerals* **2022**, *12*, 1161. <https://doi.org/10.3390/min12091161>

Academic Editors: Juan Manuel Martín-García, Rafael Delgado and Julio Calero

Received: 29 July 2022

Accepted: 8 September 2022

Published: 14 September 2022

**Publisher’s Note:** MDPI stays neutral with regard to jurisdictional claims in published maps and institutional affiliations.



**Copyright:** © 2022 by the authors. Licensee MDPI, Basel, Switzerland. This article is an open access article distributed under the terms and conditions of the Creative Commons Attribution (CC BY) license (<https://creativecommons.org/licenses/by/4.0/>).

## 1. Introduction

The soil is a complex open system, and its generation starts with weathering of parent material and goes on along with pedogenetic processes induced by biotic and abiotic factors. The precipitations and temperature besides the topographic features are the main factors controlling the weathering of parent material and the development of new mineral phases which could coexist with their precursor minerals [1–5]. Thus, the chemical composition varies between the parent material and the newly formed soil. The biochemical processes mediated by the plant roots and the microorganisms can amplify the compositional changes [1,3].

The mineralogical composition of parent material, its structure and texture are also important features involved in the weathering evolution trends. The soil generation takes place either by mineral dissolution or transformation with the loss and apparent gains of elements due to their different geochemical behavior during the weathering of parent material [1–3].

The soil developed on the top of crystalline rocks (residual soil), on plateau regime, without a significant addition of eroded material or deposition of aeolian particles should be developed over a long time and its present composition should be related to the parent material [4–6].

Mica schist or sericite schist respectively are considered less sensitive to weathering than other crystalline rocks (e.g., basalt and granite) due to their mineralogical composition [6–8]. More often, the fine grained cluster variety of muscovite in metamorphic rocks is

called sericite [9]. The name illite is attributed to dioctahedral 2:1 mineral in the supergene environment, where it is related to K-feldspar or plagioclase weathering and muscovite transformation [10]. Illite is also representative for the diagenetic transformation of clay minerals at a higher temperature than those specific to upper supergene environment [9].

Once the sericite passed from metamorphic to supergene conditions, significant compositional change did not necessarily occur, but the dioctahedral mineral in soil is preferentially named illite [9]. The sericite and illite XRD patterns could look similar [9] in soil bulk composition and usually their differentiation could be more or less difficult to be achieved. The minor compositional changes by the transformation of sericite to illite in soil can give rise to the characteristic peaks which make the difference between these dioctahedral 2:1 minerals. However, the peak at near 10 Å is considered characteristic for illite, while that at near 9.95 Å is more often assigned to muscovite [10].

Under acidic pH condition typical of alpine soil, the transformation of inherited sericite to illite can be promoted by  $^{VI}Fe^{2+}$  oxidation, which brings us to the K release due to a lower charge within a 2:1 structure [3]. The intensity of this transformation depends on the Fe content of sericite. Subsequently, illite can undergo transformation by the ejection of  $Fe^{3+}$ , the transfer of Al between IV to VI site, the continuous loss of K and interaction with  $Na^+$ ,  $Ca^{2+}$  and  $Mg^{2+}$  bearing-solution resulting from progressive incongruent dissolution of feldspars and chlorite transformation [3]. Thus, vermiculite and smectite phases can develop at the expense of illite by its partial or total replacement without a 2:1 structural change when soil formation advances in temperate regions [3,7,10]. The enrichment of weathering solution with cations released from less resistant and less abundant minerals inherited from mica schist (e.g., feldspar and chlorite) could have a significant contribution to illite transformation. Once the expandable minerals are found in the soil with relatively low pH (4.5–5.5), their presence implies a higher degree of weathering and transformation of parent material [3], characteristic for an upper stage of soil formation.

The behaviour of cations during soil generation being controlled by a multitude of factors (pH, ionic potential along with other soil conditions such as temperature, seasonal moisture, organic matter loading, plant nutrient requirements) [2,3,7] is responsible for the chemical changes that occur in the bulk soil composition. These changes lead to the apparent accumulation or loss of cations due to the advanced weathering of the primary material or the development of new mineral phases. For this reason, the assessment of the state of soil evolution can be reached using a series of geochemical weathering indices [5,6,11–14] which were conceived on the base of the different behavior of the cations.

The mineralogical determinations and geochemical methods regarding the weathering effects and intensity can support the soil evolution status under different conditions. The alpine soil from the Mănăila area (Eastern Carpathians) was studied according to this methodology. According to our knowledge, there are no previous published studies of the mineralogy and evolution degree of acidic alpine soil developed on metamorphic rocks from the Tg3 unit (Eastern Carpathians).

## 2. Materials and Methods

### 2.1. Study Area

The sampling area belongs to the Tulgheș (Tg) metamorphic group from the Crystalline-Mesozoic Tectonic Zone of Eastern Carpathians [15–17]. Within the Tulgheș metamorphic group, five units are known. The metamorphosed rhyolitic volcano-sedimentary Tg3 unit represents the geological setting of the Mănăila area and consists of sericite schist, quartz-sericite schist, quartz sericite-chlorite schist and rhyolitic metatuffs [16,17]. The rock-forming minerals of mica schist consist of quartz (24–70%), sericite and chlorite (12–58%), while the main accessory minerals are represented by feldspars (5–30%) and Ti bearing-minerals (0–10%) [18]. Also in the Tg3 unit, Cu-ore deposits of syngentic volcano-sedimentary origin occur as strata and lenses of massive or disseminated sulfides. The mineralization of Cu-rich pyrite is associated with chalcopyrite, sphalerite and galena and subordinately with

arsenopyrite, pyrrhotite, tetrahedrite, bournonite and ilmenite [15,18–20]. The open-pit extraction of ore-deposit from Mănăila is still active (Figure 1).

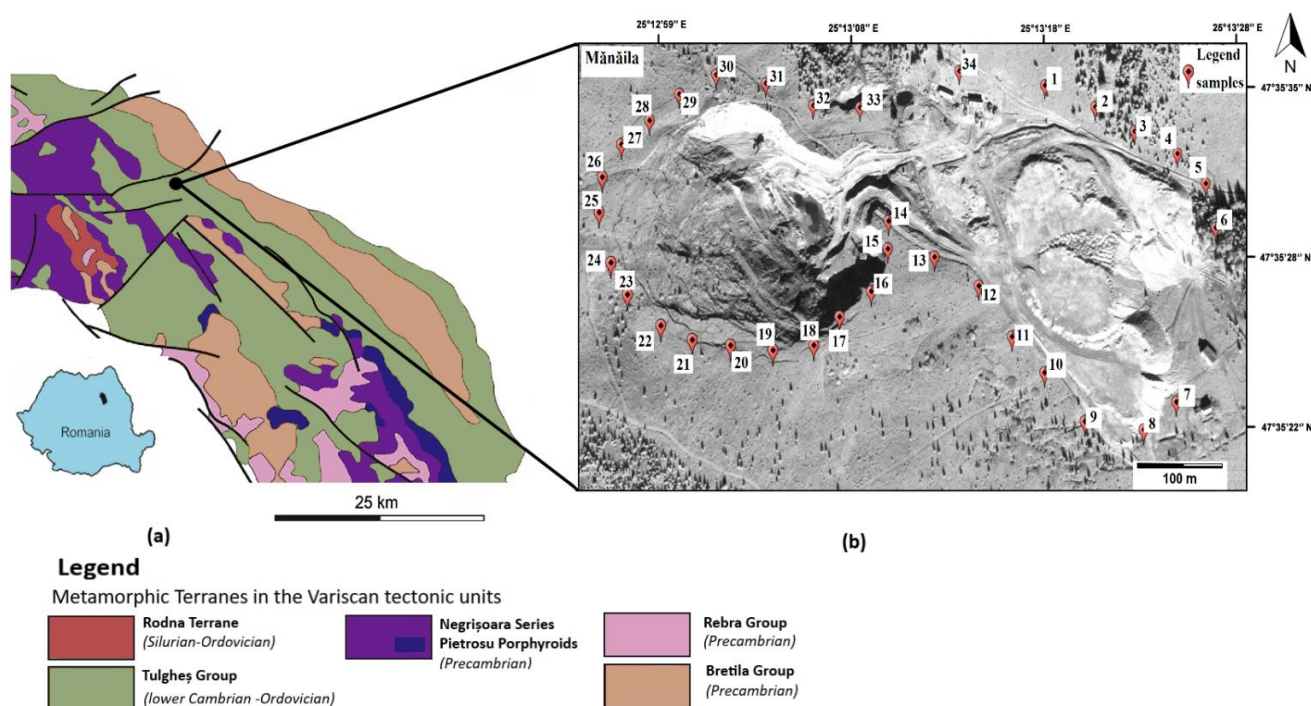


**Figure 1.** The Mănăila open-pit exploitation (a) geological map of the area, modified after [21] and (b) soil samples location using Google Map as base maps [22].

The alpine climate conditions are determined by altitude (about 1230 m), humidity (maximum in June and July; 105 mm rain/month in average), dryness (from October to March with 35 mm precipitation/month) and temperature (16.3 °C in average during summer; −5.5 °C in average during winter).

## 2.2. Soil Sampling and Preparation

A total of 34 soil samples were collected around the Mănăila open-pit (Figure 1). The topographic features of area around the open-pit are typical of the alpine plateau and the vegetation cover is dominated by lingonberry (*Vaccinium vitis-idaea*) an ever green dwarf shrub. The depth of sampling was 0–20 cm and the soil preserved in ziplock bags was dried in the lab at 40 °C and sieved to <2 mm grain fraction. The grains size was then reduced to finer powder in a mechanical mill equipped with two agate jars and agate balls (30 min and 1000 rpm). Thus, much more homogenous grain size samples were obtained for mineralogical and chemical analyses.

## 2.3. Soil Analyses

The mineralogical composition of bulk soil samples was performed by XRD, FTIR and SEM-EDS methods, whereas the bulk chemical composition was assessed by ED-XRF method.

X-ray diffraction patterns were recorded using a Bruker D8 Advance automated diffractometer (Karlsruhe, Germany) with vertical goniometer, Cu K $\alpha$  radiation and Ni filter. The voltage of 40 kV and the beam current of 40 mA were applied. The random orientated samples were scanned in the range 4–90°2 $\theta$ , with a step size of 0.04°2 $\theta$  and 4 s/step. The divergent slit was 0.6 mm and the detector slit was 0.2 mm. Qualitative and quantitative mineral contribution to the bulk soil composition was completed with the software program DIFFRAC.EVA v.3.1 (profile fitting based software). The mineral species were identified on the base of characteristic relative intensities and positions of the peaks

fitting the information from the ICDD database (version 2.1302/software version 4.13.3.6) (2013) [23].

The infrared absorption spectra of bulk soil were collected with the FTIR-Bruker Tensor 27 Spectrometer (BRUKER Optic, GmbH, Ettlingen, Germany). In order to identify the presence of different clay minerals, each sample was scanned in the range from 400 to 4000  $\text{cm}^{-1}$  with a resolution of 2  $\text{cm}^{-1}$ . Prior to FTIR analysis, 1 mg of the mechanically grounded samples were mixed and homogenized with 149 mg of dry KBr and transformed to pressed pellets under 9  $\text{t}/\text{cm}^2$  in a hydraulic press.

The bulk soil particles were observed using a Hitachi TM3030 Plus Scanning electron microscope (SEM) (Hitachi High-Techologies Corporation, Tokyo, Japan) and analyses with Bruker Quantax 70 dispersive X-ray spectrometer (EDS) (BRUKER Optic, GmbH, Ettlingen, Germany). The operating conditions included 15 kV acceleration voltages and 10 nA beam current. The exposure time was reduced to 30 s in order to avoid possible damage of particle (especially the loss of K and Na). The structural formulas of dioctahedral 2:1 minerals were calculated on the base of 22 theoretical total charge in anhydrous state, using the cationic abundance set out in atomic percent [24] and literature quoted therein. Since the EDS analyses do not make the difference between iron oxidation states, the total Fe content was attributed to trivalent specie. The distribution on structural sites was achieved according to Churchman and Verde (2019; and literature quoted therein) [3].

Prior to performing the chemical analysis of bulk soil by the ED-XRF method, pressed pellets of 9 g in weight were prepared mixing sample and blind powder (5:1). More details about pellets preparation are presented elsewhere [25,26]. The standardization was achieved by using Certified Reference Materials (SO1-4, RT, RTH, GSD and LKSD). Each sample was exposed twice, and the final results represent the arithmetic average.

#### 2.4. Methods of Geochemical Data Interpretations

The soil evolution degree was studied by the means of weathering indices described in the literatures [5,6,11–14,27]. Most of these indices are conceived as molar ratios among elements with different mobility during silicate weathering. Since the same element could be associated with several mineral types, its distribution among them should be previously checked. More often, there is a greater possibility in the case of CaO to be present in different minerals such as carbonates, phosphates and silicates. In the Mănăila soil, the CaO distribution among carbonate, apatite and silicates ( $\text{CaO}^*$ ) was not possible for two reasons: (i) acidic pH and very low CaO% content do not fulfill the conditions of secondary carbonate existence; (ii) high  $\text{P}_2\text{O}_5$  content sometimes requires a higher CaO than is found in soil. Thus, the  $\text{CaO}^*$  corresponding to silicates was attributed to total molar CaO from analyses.

The most popular index CIA—chemical index of alteration (Equation (1)) applied on soil maturity studies considers the loss of mobile elements in relation with aluminum oxide assumed to be the most important and abundant immobile elements during weathering [12,28]:

$$\text{CIA} = (\text{Al}_2\text{O}_3 \times 100)/(\text{Al}_2\text{O}_3 + \text{CaO} + \text{Na}_2\text{O} + \text{K}_2\text{O}) \quad (1)$$

For fresh materials, CIA takes values lower than 50. Weathered materials are divided in three main categories: 50–65 weak weathered, 65–85 moderate or intermediate weathered and 85–100 intensive or strong weathered [13].

Plagioclase index of alteration (PIA) (Equation (2)) [13] excludes  $\text{K}_2\text{O}$  from the CIA formula because of non-consistent behavior of K during supergene K-feldspar weathering. In the Mănăila soil parent material, the plagioclase contribution is limited and their presence in soil would reflect a low degree of evolution.

$$\text{PIA} = [(\text{Al}_2\text{O}_3 - \text{K}_2\text{O}) \times 100]/(\text{Al}_2\text{O}_3 + \text{CaO} + \text{Na}_2\text{O} - \text{K}_2\text{O}) \quad (2)$$

Another popular index of weathering (WIP) was proposed by Parker (1970) [11]. WIP is based only on mobile elements content in relation with their relative bond strength with oxygen (Equation (3)). This index was found to be representative for weathered

felsic heterogeneous metamorphic rock [6]. The low values point out a higher degree of weathering, whereas high values are typical of slightly weathered material.

$$\text{WIP} = (\text{CaO}/0.7) + (2 \times \text{Na}_2\text{O}/0.35) + (2 \times \text{K}_2\text{O}/0.25) + (\text{MgO}/0.9) \times 100 \quad (3)$$

In order to include the variation of silica from parent material to soil, the weathering intensity scale (WIS) by Meunier et al. (2013) [14] was considered. Besides classical mobile and immobile cations, Si, Mg, Fe<sup>2+</sup> and Fe<sup>3+</sup> are considered for assessment of weathering intensity. The error induced by the use of Fe<sub>2</sub>O<sub>3</sub> as total iron content is minimal for felsic compositions and oxidizing condition typical of soil [14]. This method is based on monocationic millimoles (mMol).

Herein, the ternary M<sup>+</sup>-4Si-R<sup>2+</sup> system was used, where:

$$\begin{aligned} R^{2+} &= \text{mMolFe}^{2+} + \text{mMolMg}^{2+} + \text{mMolMn}^{2+}; \\ M^+ &= \text{mMolNa}^+ + \text{mMolK}^+ + 2\text{mMolCa}^{2+}; \\ 4\text{Si} &= \text{mMolSi}/4 \text{ (Si amount corresponding to the general formula unit of phyllosilicates)} \end{aligned}$$

### 3. Results

#### 3.1. Soil Mineralogy

The XRD patterns of the bulk soil samples show a relative uniform mineralogical composition. The main minerals are represented by quartz (Q), dioctahedral 2:1 minerals, Na-plagioclase (Ab) and chlorite (Table 1).

**Table 1.** The main soil minerals-quantitative (%) mineral composition (XRD).

	Qtz	DM	Na—Plg	Chl	Σ (Mica + Chl)
S3	33.65	38.06	21.56	6.72	44.78
S5	40.04	41.42	13.18	5.37	46.79
S7	31.99	41.45	17.34	9.22	50.67
S10	37.98	47.48	6.01	8.52	56
S15	32.47	36.08	10.95	20.5	56.58
S21	27.47	59.76		12.77	72.53
S28	42.24	39.13	14.18	4.45	43.58
S30	16.35	53.49	20.9	9.26	62.75

Qtz: quartz; DM: dioctahedral 2:1 minerals; Na—Plg: sodium—plagioclase; Chl—chlorite.

Dioctahedral 2:1 minerals exceeded quartz contribution, both minerals comprising over 70% of soil bulk mineral composition. The abundance of Na-plagioclase was higher than that of chlorite (either as ferroan or as ferrian clinocllore) in all samples. Quantitatively, phyllosilicates (dioctahedral 2:1 minerals and chlorite) were the dominant minerals, since their contribution to the soil composition range between 45 to 73%.

Quartz, Na-plagioclase and chlorite were considered as primary minerals as long as they are rock-forming minerals of the parent material represented by mica-schist from the Tulgheş Group (Tg3 unit). Dioctahedral 2:1 minerals in parent material occurred in fine grained clusters called sericite [18]. Generally, sericite with high resistance to weathering can undergo characteristic transformation processes over a very long period of time [1,3,4,10]. The newly formed dioctahedral 2:1 minerals such as illite and the expandable clay minerals (e.g., vermiculite, smectite or mixed layered minerals) [1,3,9] are expected to be found in soil and their abundance can be used as index for the soil evolution stage.

The XRD pattern of soil bulk samples that were not necessary make up the differences among new dioctahedral phases. However, the literature references e.g., [3,29–31] offer

the characteristic peaks for illite and vermiculite like clay mineral determined on the bulk clay fraction (2  $\mu\text{m}$ ) of soil. Thus, the high intensity peaks to 10  $\text{\AA}/8.730^\circ 2\theta$ , 5  $\text{\AA}/17.70^\circ 2\theta$ , 4.46  $\text{\AA}/19.85^\circ 2\theta$ , 3.34  $\text{\AA}/26.60^\circ 2\theta$  infer the presence of illite, whereas the peak from 6.2 $^\circ 2\theta$  is considered representative for vermiculite.

Extrapolating from the XRD patterns of bulk clay fraction (<2  $\mu\text{m}$ ) to those of the soil bulk mineralogy (<2 mm), some observations can be taken out. In the Mănăila spectra, the high intensity reflection at 10  $\text{\AA}$  was identified for most of the samples (Table 2) and it could be attributed to illite. Other characteristic peaks were also found at 4.46  $\text{\AA}$  and 3.34  $\text{\AA}$ , suggesting the contribution of illite to soil mineralogy.

**Table 2.** d-spacing ( $\text{\AA}$ )/ $^\circ 2\theta$  characteristic peaks for illite according to reference materials and within Mănăila bulk soil.

002-0050 *	01-078-5138 *	S3	S5	S7	S10	S15	S21	S28	S30
10.000/ 8.836	10.0221/ 8.816	9.951/ 8.879	10.001/ 8.835	9.979/ 8.854	10.015/ 8.823	9.984/ 8.85	10.005/ 8.831	10.099/ 8.748	9.989/ 8.845
4.460/ 19.891	4.459/ 19.896	4.470/ 19.844	4.488/ 19.896	4.476/ 19.821	4.469/ 19.848	4.487/ 19.769	4.497/ 19.792	4.553/ 19.487	4.522/ 19.613
3.330/ 26.750	3.348/ 26.604	3.342/ 26.655	3.347/ 26.615	3.343/ 26.643	3.346/ 26.607	3.344/ 26.369	3.348/ 26.606	3.334/ 26.713	3.321/ 26.821

\* ICDD reference patterns for illite.

A few peaks near 3.5  $\text{\AA}$  and 2.55  $\text{\AA}$  were assigned to muscovite, which were inherited from parent material and underwent very limited transformation during soil formation (Figure 2).

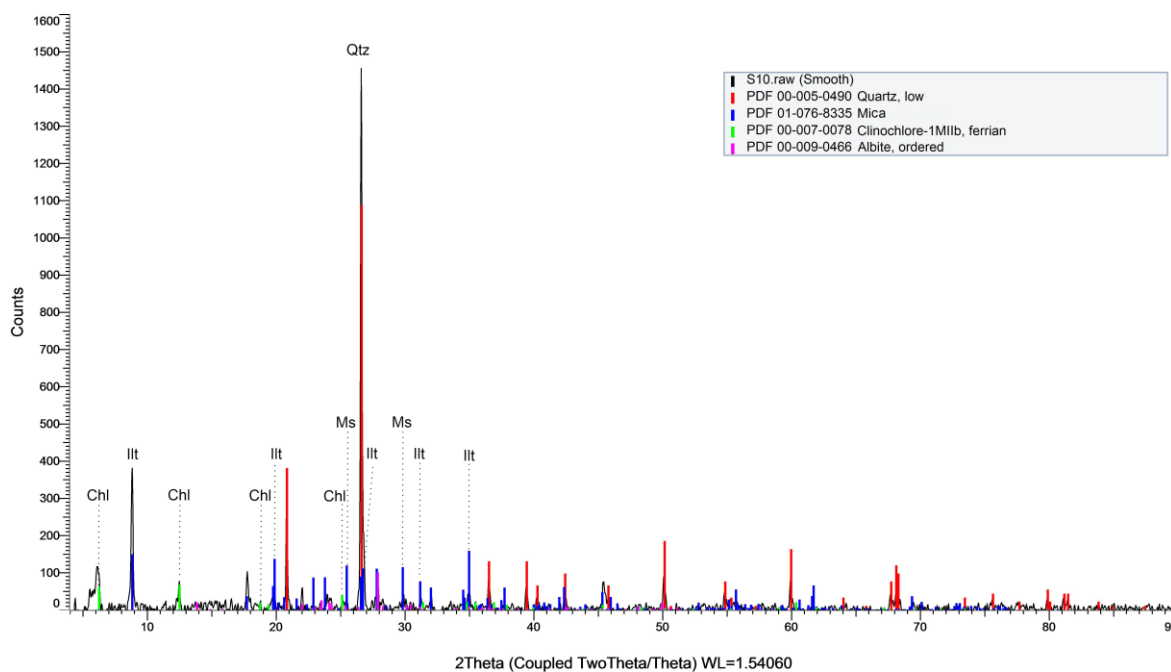


**Figure 2.** An X-ray powder pattern for a representative sample of soil from Mănăila.

Chlorite in bulk soil composition was identified using the characteristic peak [32] at 14.2  $\text{\AA}/6.230^\circ 2\theta$ , 7.1  $\text{\AA}/12.460^\circ 2\theta$ , 4.71  $\text{\AA}/18.730^\circ 2\theta$  and 3.53  $\text{\AA}/25.060^\circ 2\theta$  (Figure 2). The compositional trend of chlorite solid solution was also pointed out by comparison between odd and even order reflection intensities. Within the XRD pattern of chamosite end-member, the odd order reflections (at near 14.2  $\text{\AA}$  and 4.71  $\text{\AA}$ ) are lower than even order reflections (at near 7.1  $\text{\AA}$  and 3.53  $\text{\AA}$ ) [32–34]. For the clinochlore end-member, the odd

and even order peak intensities are stronger; the differences between intensities are not so high compared with chamosite [32–34]. For chlorite in the Mănăila soil, the even order reflections (at near 7 Å and 3.55 Å) and odd order reflections (14.2 Å and 4.71 Å) intensities were close to each other.

These narrow differences between even and odd-order peaks denoted that chlorite was represented mainly by clinochlore, whereas chamosite contribution to solid solution was limited for most of the samples, with one exception for which higher even order reflections were found (S15) (Figure S1—supplementary material).

The FTIR analyses were performed in order to gain supplementary information about soil mineralogy. Generally, the dioctahedral 2:1 minerals in soil do not show a unique or ideal composition and more often they can be represented by dioctahedral 2:1 mixed layer minerals such as illite-vermiculite or illite-smectite [3,35].

The absorption bands of muscovite, illite, expandable clay minerals (including mixed layered minerals), kaolinite, chlorite, quartz and organic matter as well were searched on each spectrum according to their characteristic vibration peaks [36–40]. The similarities among spectra were good. The minor differences concerning the peaks intensity and position (wavenumber) were related to the mineral abundance and compositional variability.

Along with XRD determinations, FTIR analyses confirmed and also provided details upon the mineralogy of the soil fraction smaller than 2 mm (Figure 3). The clear absorption bands at near  $3621\text{ cm}^{-1}$  (vibration from OH stretching), together with the weak peak at  $1010\text{ cm}^{-1}$  (due to Si-O stretching) and  $912\text{ cm}^{-1}$  (vibration of Al-OH-Al bending) were assigned to illite as dominant dioctahedral-2:1 minerals component [37–40]. The weaker peak at about  $830\text{ cm}^{-1}$  was attributed to the Al-OH-Mg vibrations and correspond to mixed layered minerals resulting either from illite transformation to vermiculite (where Mg substitute for Al) or chlorite transformation (illite-smectite mixed layers) [38,40]. The characteristic bands for adsorbed water in interlayer spaces were identified at near  $3420\text{ cm}^{-1}$  and  $1640\text{ cm}^{-1}$ ; it was related to expandable clay minerals which can be included in the clay mixed layered minerals [36,38,40].

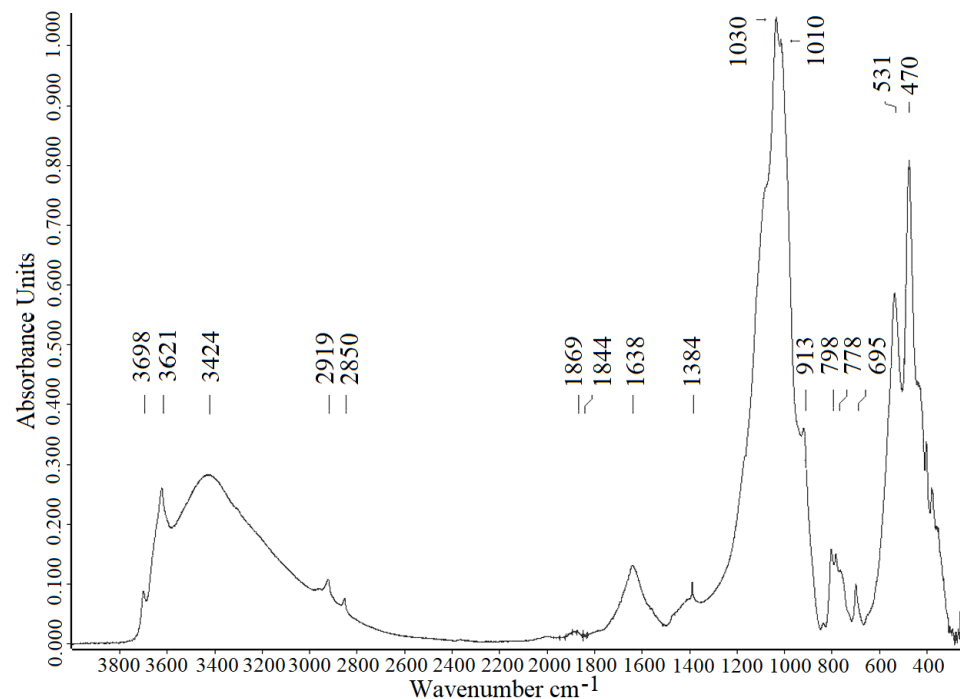


**Figure 3.** FTIR spectra for the representative sample of soil from Mănăila.

The vibration peaks at near  $530\text{ cm}^{-1}$  (Si-O-Al bending) and  $472\text{ cm}^{-1}$  (Si-O-Si bending) plus  $753\text{ cm}^{-1}$  (Si-O-Al stretching) in some samples were also assigned to illite and illite-vermiculite [35,36,39].

The minor contribution of kaolinite could have been considered from the OH-stretching vibration near  $3698\text{ cm}^{-1}$  [37,38,40], significantly weaker than the peak at near  $3620\text{ cm}^{-1}$ . However, kaolinite was not detected via XRD method on bulk soil composition. The vibration at near  $3698\text{ cm}^{-1}$  better reflected the chlorite presence [41] which was confirmed by XRD. Additionally, the vibration at near  $1030\text{ cm}^{-1}$  and  $650\text{ cm}^{-1}$  in some samples was also considered representative for chlorite [42,43].

On the FTIR spectra, the Si-O stretching band at near  $800\text{ cm}^{-1}$ ,  $780\text{ cm}^{-1}$  and  $695\text{ cm}^{-1}$  were assigned to quartz [35,37]. This mineral, with high proportion in soil according to XRD quantitative determination, is characterized by the same Si-O stretching bands as illite. Herein, dealing with <2 mm fraction of soil, the vibration values mentioned above were preferentially attributed to quartz.

The characteristic vibrations of organic matter do not overlap those of the octahedral 2:1 minerals or quartz. Thus, the peaks at near  $3300\text{ cm}^{-1}$ ,  $2925\text{ cm}^{-1}$ ,  $2850\text{ cm}^{-1}$  and  $1384\text{ cm}^{-1}$  [35,37] were consistent with the vibration of C-H bond in  $-\text{CH}_3$  and  $-\text{CH}_2-$  radicals or C-OH deformation in  $-\text{COOH}$  radical. All these radicals are found in soil organic acids and in untreated samples they have to be an ordinary component of soil.

The mineralogical composition was completed with SEM-EDS analysis. Among minerals already identified by XRD, the Ti-bearing minerals such as ilmenite and rutile were also found. These accessory minerals were indubitably inherited from the soil parent material (mica schist of  $\text{Tg}_3$  unit). The examinations of dioctahedral 2:1 minerals by EDS pointed out some compositional differences among investigated particles. Their chemical composition was mainly related to Si, Al, K and subordinated to Fe and Mg. The presence of Ti and Na was noted to be only isolated (Table 3).

**Table 3.** The EDS chemical composition of dioctahedral 2:1 minerals.

Atomic (%)	S3_1	S5_1	S7_1	S10_1	S10_4	S15_1	S21_1	S28_1	S30_1
O	64.07	63.87	63.39	67.3	66.09	60	67.39	64.12	63.67
Si	18.25	17.78	16.62	16.39	14.97	17.79	14.53	16.02	16.75
Al	14.21	13.3	14.65	11.48	13.45	16.06	12.74	14.07	14.32
Fe	0.63	1.04	0.77	0.92	0.87	0.89	0.91	0.86	0.21
Mg		0.98	0.64	1.31		0.55	0.66	0.54	0.83
K	2.65	2.76	3.94	2.59	3.73	3.95	3.97	3.63	4.08
Na					0.89	0.79		0.76	
Ti		0.28							
Structural formula									
<sup>IV</sup> Si	3.34	3.26	3.1	3.34	3.07	3.06	3.07	3.08	3.17
<sup>IV</sup> Al	0.66	0.74	0.9	0.66	0.95	0.94	0.93	0.92	0.83
<sup>VI</sup> Al	1.94	1.70	1.83	1.68	1.82	1.82	1.75	1.79	1.88
<sup>VI</sup> Fe	0.12	0.19	0.14	0.19	0.18	0.15	0.19	0.17	0.04
<sup>VI</sup> Mg		0.18	0.12	0.27		0.10	0.14	0.10	0.15
<sup>VI</sup> Ti		0.05							
Sum VI	2.06	2.12	2.09	2.13	1.99	2.07	2.09	2.06	2.07
<sup>XII</sup> K	0.49	0.51	0.73	0.53	0.76	0.68	0.82	0.70	0.77
<sup>XII</sup> Na					0.18	0.14		0.15	
Sum XII	0.49	0.51	0.73	0.53	0.95	0.82	0.82	0.85	0.77
Charge									
XII site	0.49	0.51	0.73	0.53	0.95	0.82	0.82	0.84	0.77
IV site	-0.66	-0.74	-0.90	-0.66	-0.94	-0.94	-0.93	-0.92	-0.83

**Table 3.** *Cont.*

Atomic (%)	S3_1	S5_1	S7_1	S10_1	S10_4	S15_1	S21_1	S28_1	S30_1
VI site	0.17	0.23	0.17	0.13	−0.01	0.12	0.12	0.07	0.06
IV + VI sum	−0.49	−0.51	−0.73	−0.53	−0.95	−0.82	−0.82	−0.85	−0.77
	Sme *	Sme *	Ilt-Vrm *	Sme *	Ms *	Ilt *	Ilt *	Ilt *	Ilt-Vrm *

\* mineral symbols according to IMA—CNMNC [44]: Sme—smectite, Ilt—illite; Vrm—vermiculite; characteristic charge deficit: (1) 0.9–0.75 for Ilt; (2) 0.75–0.6 for Vrm; (3) 0.6–0.2 for Sme [1,3].

The distribution of cations on structural sites showed that there is a slight octahedral excess and a variable interlayer deficit (Table 3). The deviation from theoretical cations occupancy in octahedral position (>2 apfu) inferred the presence of more than one component within the investigated dioctahedral 2:1 minerals [29,41]. This feature agreed with FTIR determinations, revealing the presence of mixed-layer minerals.

The dominant component was also considered according to the charge of 2:1 layer (Table 3). The charge deficit around −0.50 per formula unit (apfu) (Table 3) fitted to the characteristic charge range of smectite (0.2–0.6) [1]. These smectite dominant 2:1 structures showed lower <sup>XII</sup>K (≈0.5 apfu) plus higher <sup>IV</sup>Si (3.25 apfu) and <sup>VI</sup>(Mg+Fe<sup>3+</sup>) (0.45 apfu) (Table 3). These samples with low K and no detectable Na and Ca, but with higher Fe and Mg, were attributed to a chlorite precursor.

The illite dominant layers coexisting with vermiculite layers were identified by the charge deficit between 0.77–0.73 apfu, whereas illite was considered to have a charge deficit between 0.8 and 0.9 (Table 3). In both situations, the K was relatively high (0.68–0.82 apfu) and Si was between 3.1 and 3.06 apfu. The contribution of <sup>VI</sup>(Mg+Fe<sup>3+</sup>) was not negligible (0.25–0.33 apfu), suggesting the ability of these two cations with high mobility to substitute for Al in octahedral site since the 2:1 precursor preceded its transformation.

According to EDS analyses, muscovite was found only in a single sample. The charge deficit in this case is higher, attaining −0.95 per formula unit (Table 3). The presence of muscovite among dioctahedral 2:1 minerals was in agreement with XRD results.

### 3.2. Soil Geochemistry

The geochemical results on bulk soil composition were shown as basic statistic parameters in Table 4. Silica and alumina accounted for more than 68% of the bulk composition of considered soil (Table 4). In parent material (sericite schist), SiO<sub>2</sub> and Al<sub>2</sub>O<sub>3</sub> exceeded 70% with an average value of 85.51% which support their provenance from a felsic composition precursor (protolith). Among alkali and alkali earth elements in soil, K<sub>2</sub>O prevailed over MgO > CaO > Na<sub>2</sub>O (Table 4).

**Table 4.** The basic statistical parameters for the geochemical composition of soil and parent material.

Basic Statistic	SiO <sub>2</sub>	TiO <sub>2</sub>	Al <sub>2</sub> O <sub>3</sub>	Fe <sub>2</sub> O <sub>3</sub>	MgO	MnO	CaO	Na <sub>2</sub> O	K <sub>2</sub> O	P <sub>2</sub> O <sub>5</sub>	pH
Soil (n = 34)											
average	52.67	0.85	20.20	8.31	0.89	0.09	0.24	0.52	3.93	0.22	4.64
median	52.11	0.94	20.32	8.75	0.83	0.06	0.23	0.11	3.89	0.23	4.59
min	46.95	0.51	16.53	4.77	0.47	0.02	0.18	0.01	3.54	0.10	4.08
max	59.43	1.07	26.46	11.89	1.50	0.22	0.36	4.52	4.50	0.34	5.53
CVR%	5.95	24.25	9.16	30.42	41.32	137	19.94	416	3.79	40.61	
Parent material (n = 20)											
average	72.56	0.21	12.95	7.06	1.67	0.05	0.33	2.91	1.28	0.04	-
median	73.90	0.07	13.80	2.40	1.35	0.03	0.15	2.80	1.30	0.02	-
min	55.20	0.03	4.50	1.20	0.45	0.00	0.01	1.20	0.36	0.01	-
max	85.10	0.88	20.70	30.90	4.50	0.27	1.80	5.30	3.10	0.18	-
CVR%	7.12	52.19	18.80	64.86	57.11	98.84	127.81	92.38	39.71	49.92	-

The distribution of elements in soil of the Mănăila area was studied based on the CVR parameter (% robust coefficient of variation) (Table 4). Thus, elements such as K, Si and Al showed a homogeneous distribution for which CVR was less than 10%; elements such as Ca,

Ti, Fe had a relatively homogeneous distribution for which CVR was between 10 and 30%; elements such as Mn and Na had a very inhomogeneous distribution for which CVR was more than 100%. The very pronounced variation of Na content in soil suggested that the Na source is not uniformly distributed. Moreover, XRD analyses confirmed the variation of the Na feldspar contents in the investigated samples (Table 1), which directly reflected in the non-homogeneous distribution of Na in soil. This non-homogeneous distribution of Na was amplified in soil comparing with the parent material (Table 4). CVR (%) for Na increased four times in soil compared with the parent material. The Ca distribution according to CVR (%) (Table 4) significantly lowered from parent material to soil, from highly non-homogeneous to relatively homogeneous. The Mg distribution in soil was close to relatively homogeneous, decreasing from the parent material to soil.

#### 4. Discussion

The geochemistry of soils is mainly related to its mineralogy and subordinately to pedogenetic processes induced by plant–soil interactions. Therefore, the relationships that develop between the major elements can reflect soil mineralogy and the effects of supergene alteration upon soil generation.

Generally, the increase of clay mineral contribution to the soil mineralogical composition is reflected by the apparent changes of major oxides contents from parent material to soil. Thus, in the soil from Mănăila area, the apparent concentration increases of  $\text{Al}_2\text{O}_3$  and  $\text{K}_2\text{O}$  accompanied by both the minimal decrease of  $\text{CaO}$  and the significant lowering of  $\text{Na}_2\text{O}$  (and  $\text{MgO}$ ) (Table 4) was attributed to the soil clay-minerals development and their preference for K and Ca [45]. The  $\text{K}_2\text{O}/\text{Al}_2\text{O}_3$  ratio (weight%) [46] can serve for the identification of the dominant dioctahedral 2:1 minerals. This ratio decreases from muscovite (0.33) to illite (0.30–0.20) and vermiculite (0.11–0.06), respectively. The ratio range (0.25–0.15; 0.20 in average) found in Mănăila soil supported the dominance of illite in soil mineralogy.

Once the high illite contribution was considered by the means of soil bulk composition and confirmed by mineralogical investigations, a good relation between  $\text{K}_2\text{O}$  and  $\text{Al}_2\text{O}_3$  could be expected. The absence of correlation between  $\text{K}_2\text{O}$  and other major ions (Table S1—supplementary material), especially  $\text{Al}_2\text{O}_3$  and  $\text{Fe}_2\text{O}_3$ , was assigned to the influence of biological recycling of K as nutrient [47]. Plant roots uptake and deposition can significantly modify the mobility and concentrations of nutrients in the rhizosphere [3,47,48]. The Mănăila soil samples were collected from the first 20 cm of soil which comprise this fluctuation zone in the soil. The correlation of  $\text{Al}_2\text{O}_3$  and  $\text{Fe}_2\text{O}_3$  ( $r = 0.55$ ) was attributed to a common source such as dioctahedral 2:1 minerals or Fe oxy-hydroxide coating on them. However, the relation of  $\text{Fe}_2\text{O}_3$  with  $\text{P}_2\text{O}_5$  ( $r = 0.76$ ) suggested the association of these elements within a common source. This could have been possible under low pH conditions, when the leached  $\text{Fe}^{3+}$  from 2:1 minerals could have precipitated with P from soil solution to form secondary phosphate mainly as coatings on other mineral grains [49]. Additionally, the P adsorption on  $\text{Fe}^{3+}$  oxy-hydroxides, even if was limited [50], could have enhanced the correlation of  $\text{P}_2\text{O}_5$  with  $\text{Fe}_2\text{O}_3$ .

The relation of molar ratios between of K/Al and Si/Al (Figure 4a) with good positive correlation ( $r = 0.85$ ) denoted that Al enrichment was accompanied by K and Si depletion. This trend can result from the transformation of illite to vermiculite possibly within mixed layered 2:1 structures which were confirmed by SEM-EDS results on individual grains. The existence of illite-vermiculite mixed layers was also supported by the vibration peaks at near  $530\text{ cm}^{-1}$ ,  $472\text{ cm}^{-1}$  and sometimes at near  $753\text{ cm}^{-1}$  [35,36,39].

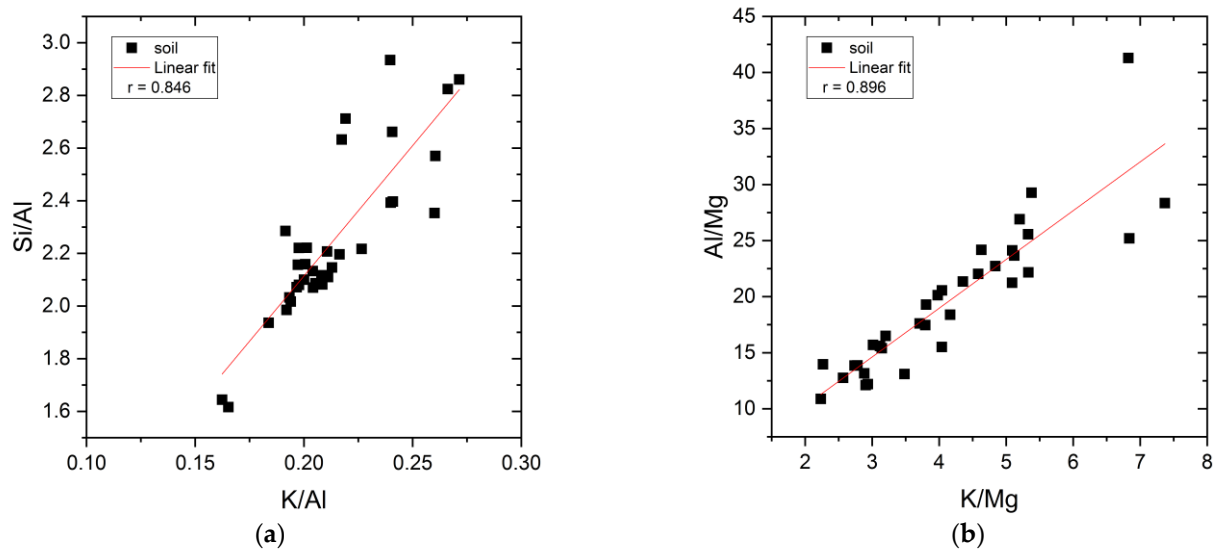


**Figure 4.** (a) K/Al:Si/Al molar ratio correlations (b) K/Mg:Al/Mg molar ratio correlation.

The good relation between K/Mg and Al/Mg molar ratios ( $r = 0.90$ ) (Figure 4b) in soil could be related to the chlorite weathering products. Chlorite was found within soil mineral composition (Table 1), but the increase of K/Mg and Al/Mg molar ratios from parent material (K/Mg = 0.31–3.29; Al/Mg = 3.12–11.12) to soil (K/Mg = 2.23–7.37; Al/Mg = 10.41–41.28) inferred the Mg loss during weathering. Thus, part of the inherited chlorite transformed (due to its higher sensitivity) to 2:1 dioctahedral minerals and most possible to smectite as the good correlation of Si/Mg and Al/Mg molar ratios ( $r = 0.87$ ) also denoted (Figure S3—supplementary material). Smectite was identified by SEM-EDS analysis, whereas FTIR investigation confirmed the presence of expandable minerals within mixed layered structures by characteristic vibrations at near  $3420\text{ cm}^{-1}$  and  $1640\text{ cm}^{-1}$  [36,38,40].

The chlorite dissolution and transformation to smectite and also the development of illite-vermiculite mixed layers under cold and rainy climate conditions could be promoted by organic acids found in soil [3,8]. Over time, the vegetation cover enhanced and now it consists of lingonberry shrubs (*Vaccinium vitis-idaea*) and acidophile herbs (*Luzula silvatica*, *Soldaella montana*). The organic acids formed from plant debris and roots deposition in the soil could have interacted with the mineral fraction and amplified weathering effects. On the FTIR spectra, the presence of organic acids was detected through the peaks at near  $3300\text{ cm}^{-1}$ ,  $2925\text{ cm}^{-1}$ ,  $2850\text{ cm}^{-1}$  and  $1384\text{ cm}^{-1}$  [35,37]. However, their clear contribution to the soil development could be better evaluated only in soil affected by podsolization [7,8,30]. The lack of evidence of podsolization processes did not allow for an accurate assessment of the involvement of organic acids in Mănăila pedogenesis.

The extent of the weathering processes responsible for soil development upon parent material could be quantified by different methods, but more often the indices using molar ratios are applied.

The weathering index of alteration (CIA) [12] (Equation (1)) is by far the most used. It presumes that feldspar weathering is the main source of mobile elements, since these minerals have the highest abundance in the upper crust and are more sensitive to weathering than dioctahedral micas [14,28,51,52]. In the Mănăila context, the low concentration of Na and Ca in soil can be related to the limited load of feldspars in parent material [18]. The history of pristine minerals changed from metamorphic protolith to soil in Tg3 unit and should be divided into three main stages: (1) the weathering of K-feldspar, plagioclase or muscovite from rhyolitic volcano-sedimentary protolith followed by diagenesis was responsible for illite generation; (2) then, the metamorphic processes gave rise to the formation of fine grained 2:1 minerals like sericite; (3) eventually, the weathering of sericite-bearing metamorphic rocks during soil formation could have resulted in both sericite partial conservation in illite and new transformation products under super-genic conditions. Thus,

CIA values in soil reflect the continued changes from pristine minerals to illite and other K-depleted clay minerals.

The mean CIA values (Table 5) indicated a moderate weathering state of soil minerals, which can be explained by the conservation trend of Al-rich composition of parent material (Table 4) reflected in soil by a high abundance of dioctahedral 2:1 minerals according to XRD data (Table 1).

**Table 5.** The weathering indices for soil and parent material.

Basic Statistic	CIA	PIA	WIP
soil			
average	78.57	92.99	41.21
median	80.31	95.59	38.10
min	58.87	62.78	34.00
max	83.49	97.78	79.50
CVR %	4.41	5.09	15.27
Parent material (rock)			
average	69.65	80.66	41.89
median	69.69	80.82	43.43
min	58.05	60.65	15.47
max	76.29	91.72	67.88
CVR %	7.13	11.46	40.31

In the A-CN-K ( $Al_2O_3$ - $CaO^*$ + $Na_2O$ - $K_2O$ ) diagram (Figure 5) [13], the samples plotted above the Plg-KFs joint (Plagioclase–K feldspar line), suggesting the low contribution of these minerals both in parent material and soil. The transition from parent material to soil was accomplished by  $Na_2O$  and  $CaO$  reduction and a minor loss of  $K_2O$ , which was emphasized by the position of samples parallel to A-CN side. Moreover, the weathering trend for both metamorphic rock and soil followed the ideal rhyolite trend [53], thus connecting the metamorphic protolith composition to soil. The soil plotting position on A-CN-K diagram (Figure 5) also denoted that the weathering processes led to an apparent  $Al_2O_3$  enrichment. The clustering of soil near the Ms-Illite joint suggested that the main mineral is still illite, kaolinite being insignificant. The lack of kaolinite or its very low abundance in soil was confirmed by XRD and FTIR analyses.

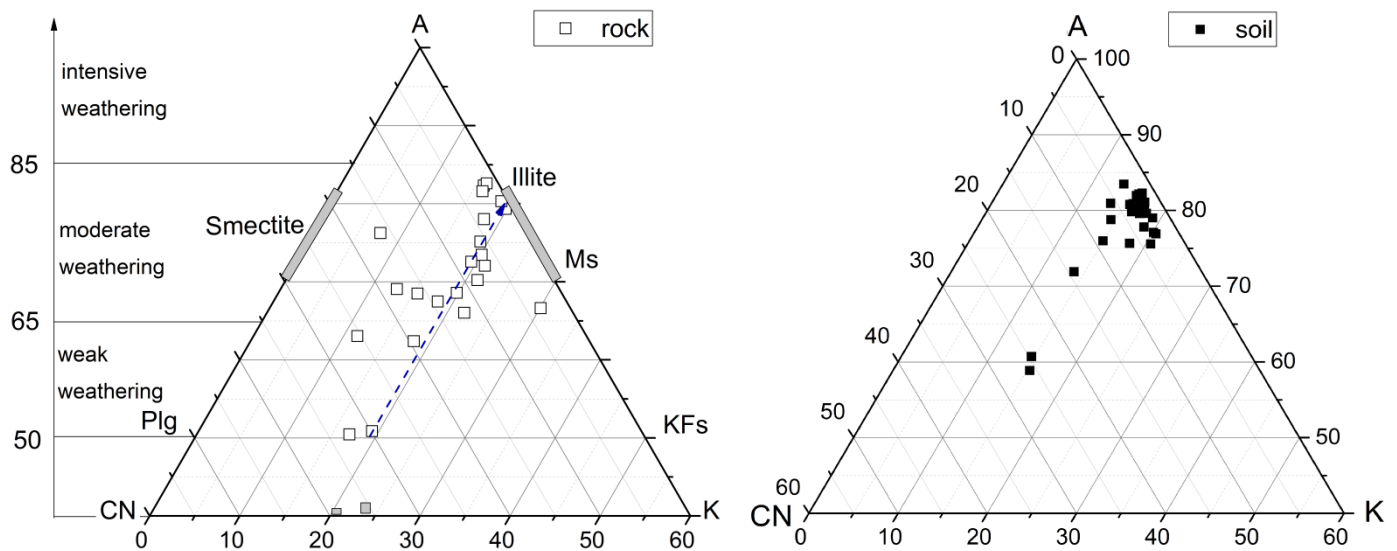


**Figure 5.** The A-CN-K ternary system [15] (Ms-muscovite, Plg-plagioclase, KFs-potassium feldspar; dashed line–rhyolite weathering trend).

The Plagioclase Index of Alteration identified for soil showed a narrow range of variation (CVR%), with most of PIA values placed above the upper limit typical of parent material (Table 5). This low increase in PIA from sericite schist to soil denotes that the soil reached an intermediate state of evolution. The PIA values could be attributed to partial Na-plagioclase dissolution in the supergene environment since a negative correlation trend (Figure S2—supplementary materials) between PIA and Na-plagioclase abundance (Table 1) was noted.

The weathering index of Parker (WIP) [11] commonly varies in reverse order with CIA. WIP for soil took values mainly between 48 and 34 (CVR% = 15.27) (Table 5) and inferred a relatively higher degree of weathering comparing with CIA, but there were no stated intervals for WIP intensity evaluation. The lower values of WIP could have been related to MgO removal in association with Na<sub>2</sub>O, CaO and K<sub>2</sub>O. However, WIP and CIA showed good correlation ( $r = 0.69$ ), which suggested that the both indices reflect the same degree for soil maturity (Figure S4—supplementary materials).

The A-CNK-FM ( $\text{Al}_2\text{O}_3\text{-CaO+Na}_2\text{O+K}_2\text{O-Fe}_2\text{O}_3 + \text{MgO}$ ) diagram (Figure 6) [12] was used in order to show how progressive Mg and Fe leaching from the minerals of the parent material enhanced whereas soil generation proceeded. The shift of the soil samples towards the A-peak (molar percentage of  $\text{Al}_2\text{O}_3$ ) could not have been explained only by the loss of Mg during weathering, because the MgO content in the parent material was low. Therefore, the partial loss of Fe was also considered to be involved and together with Mg partial loss brought to the reduction of the mafic components from the parent material to the soil. Over time under moderate acid conditions specifically to Mănăila soil, the biogeochemical processes could have overlapped with weathering, and Fe leaching and mobility to be increased. The A-CNK-FM diagram confirms the loss of Mg and Fe during soil formation.

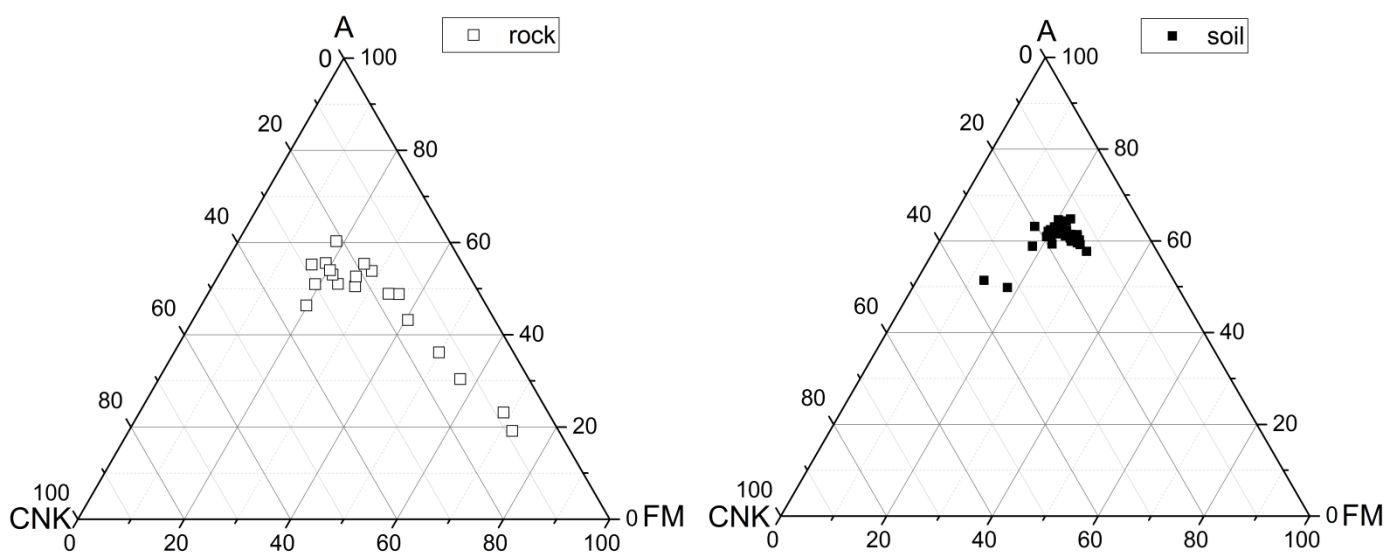
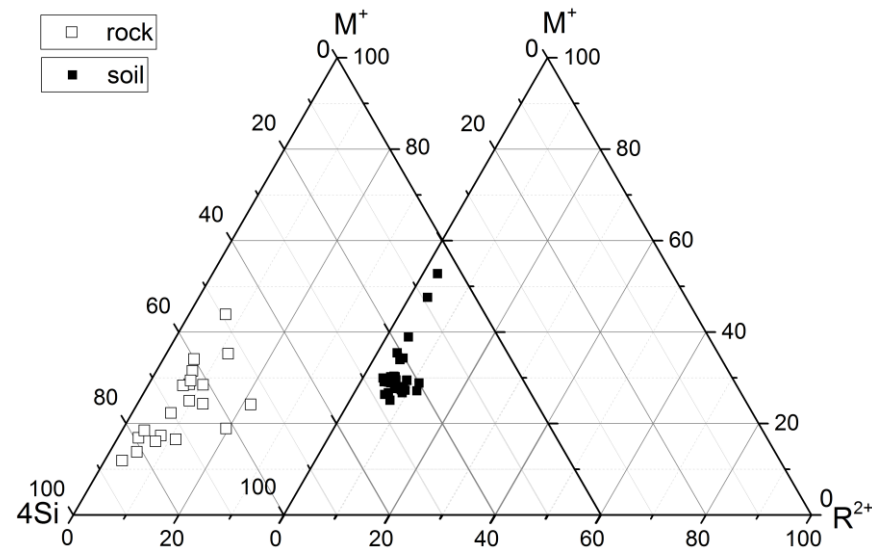


Figure 6. The A-CNK-FM diagram for parent material and soil.

During parent material weathering, the relations developed between highly mobile cations and relatively mobile Si bonded to silicates (other than quartz) can be followed applying the  $\text{M}^{+4}\text{-4Si-R}^{2+}$  system [14]. The bulk composition should reflect the apparent enrichment of Si once the Mg and Na, Ca or K cations were lost due to progressive weathering reactions which promote the generation of Si-rich minerals such as some smectite and eventually kaolinite.

For the Mănăila soil, the significant contribution of quartz in the bulk composition (Table 1) could have induced the dilution effect and thus the observations of the apparent Si gain or loss could have been disturbed. Even so, an apparent loss of Si was noted when the soil and parent material compositions were plotted within  $\text{M}^{+4}\text{-4Si-R}^{2+}$  system (Figure 7).

This trend could be explained by partial conservation of both Si and K in some soil minerals such as illite, which showed a high abundance in the soil (Table 1).



**Figure 7.** A  $M^+-4Si-R^{2+}$  diagram for rock and soil from the Mănăila area.

The composition of dioctahedral 2:1 minerals in soil could be relevant for the assessment of the soil maturity [1,9]. Thus, the dioctahedral 2:1 minerals investigated by SEM-EDS were plotted on  $M^+-4Si-R^{2+}$  diagram (Figure 8) and their distribution pointed out that there were likely two distinct types of illite within the illite compositional domain.

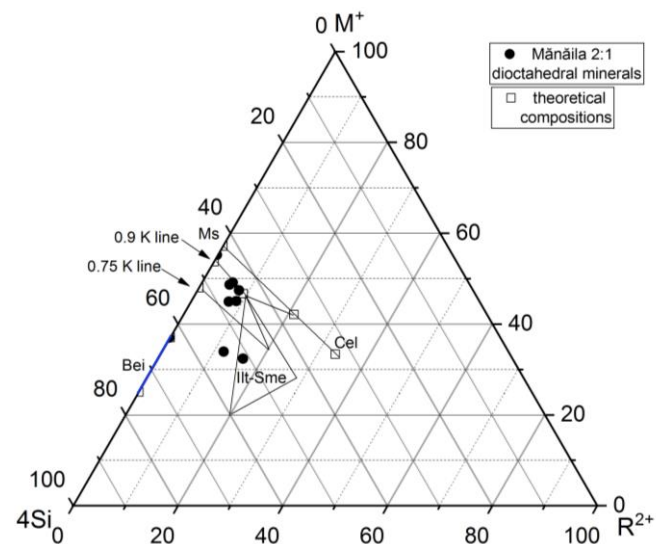


**Figure 8.** The  $M^+-4Si-R^{2+}$  system for the illite and smectite composition (Bei—beidellite; Cel—celadonite; Ill—illite; Kln—kaolinite; Sme—smectite).

The first type placed on the upper limit of illite illustrated by 0.9 K line and was considered a mixture between 2M1 and 1M polytypes [9]. The second type of illite was found between 0.9 and 0.75 K lines and was represented by 1M polytypes. The compositional domain of illit (0.9–0.75 K lines) does not include even a minor contribution of smectite (0 % smectite) [9]. The absence of Ca and the very low content of Na in illite (Table 3) confirmed the lack of smectitic component in this illite. The 2M1 polytype inferred that the higher temperature muscovite (sericite) was still preserved in soil and weathering process by transformation was limited. The 1M illite supported the presence of newly formed minerals and the weathering evolution toward a higher degree.

Besides the good separation of illite types, illite–smectite mixed layers was also illustrated on  $M^{+}4Si-R^{2+}$  diagram (Figure 8). The smectite component which is considered a commune advance weathered product in soil was probable richer in Al.

The presence of the illite compositional domain characterized by two main polytypes near smectite denoted that the weathering has not yet resulted in the generation of relatively homogeneous material. Thus, an intermediate state of the soil evolution was considered.

## 5. Conclusions

The mineralogy and geochemistry of the soil from Mănăila area revealed the effects of mica schist weathering under temperate alpine conditions. Within the bulk mineralogical composition, the dioctahedral 2:1 minerals, quartz, chlorite and Na-plagioclase were found, their abundance decreasing in this order. On the XRD spectra, the dioctahedral 2:1 minerals were considered to be represented by muscovite and, quite possibly, illite. On the FTIR vibration spectra, characteristic bands denoted that illite and mixed-layered minerals were likely to exist. SEM-EDS investigations offered more detailed information on the chemical composition of dioctahedral 2:1 minerals. Thus, illite, illite-vermiculite and smectite were found beside muscovite. Another mineral inherited from the parent material, chlorite, was also identified in the soil by XRD. Clinocllore represented the main component of the chlorite solid-solution. The FTIR determinations supported the contribution of chlorite to soil mineralogy. The identified smectite was most likely the product of chlorite transformation. The presence of chlorite and muscovite, along with two types of illite (higher and lower potassium), and mixed-layered minerals implies that the weathering of the parent metamorphic rocks has not yet generated a homogeneous material.

The main geochemical feature of the Mănăila samples was the high contributions of  $Al_2O_3$  and  $K_2O$  to soil composition. The ratio between  $K_2O/Al_2O_3$  inferred that illite was the main dioctahedral 2:1 clay mineral in the soil. The common source for  $Al_2O_3$  and  $Fe_2O_3$  was also supported by their correlation, but a certain  $Fe_2O_3$  fraction seemed to be associated with  $P_2O_5$  in secondary phosphate. The good correlation between K/Al and Si/Al molar ratios, denoting K loss and Al gain, was related to the muscovite evolution toward illite. The chlorite transformation trend was associated with the Mg loss, a process which was emphasized by the correlation of K/Mg and Al/Mg molar ratios. The chlorite evolution towards smectites was also considered based on the good correlations between Si/Mg and Al/Mg molar ratios. The weathering intensity assessment using different geochemical indices reflected a moderate degree of soil evolution as previously indicated by the mineralogical observations. The noted compositional changes due to weathering process were the apparent enrichment in Al, minor loss of K and significant depletion of Na, Mg and Ca. The loss of Mg was considered to be accompanied by a low portion of Fe more possible during chlorite transformation. The partial release of Si from some minerals also occurred. Thus, the evolution general trend supported the formation of new dioctahedral 2:1 minerals in soil at the expense of inherited muscovite from sericite schists. The initial abundance of sericite and quartz retarded soil evolution, even though organic acids were assimilated into the soil with vegetation growth and could have induced an intensification of weathering.

**Supplementary Materials:** The following supporting information can be downloaded at: <https://www.mdpi.com/article/10.3390/min12091161/s1>, Figure S1: XRD powder pattern of sample S15; Figure S2: The relation trend between PIA and Na-Plg in soil from Mănăila area; Figure S3: The relation between WIP and CIA in soil from Mănăila area; Figure S4: The relation between Si/Mg and Al/Mg molar ratios in Mănăila soil; Table S1: Correlations of major oxides of soil from Mănăila area.

**Author Contributions:** Conceptualization, D.S.S.-R., R.H. and D.-G.D.; Data curation, D.S.S.-R. and R.H.; Formal analysis, D.S.S.-R., R.H., D.-G.D. and C.O.S.; Investigation, D.S.S.-R. and R.H.; Methodology, D.S.S.-R., R.H., D.-G.D. and C.O.S.; Validation, D.S.S.-R., R.H. and D.-G.D.; Visualization, D.S.S.-R., R.H., D.-G.D. and C.O.S.; Writing—original draft, D.S.S.-R. and R.H.; writing and review, D.S.S.-R., R.H., D.-G.D. and C.O.S.; supervision and writing—review and editing: D.S.S.-R. and R.H. All authors have read and agreed to the published version of the manuscript.

**Funding:** The APC was funded by the Romanian Ministry of Research, Innovation and Digitization, within Program 1—Development of the national RD system, Subprogram 1.2—Institutional Performance—RDI excellence funding projects, contract no. 11PFE/30.12.2021.

**Data Availability Statement:** The data presented in this paper are available on request.

**Acknowledgments:** Authors are thankful to the Romanian Ministry of Research, Innovation and Digitization, within Program 1—Development of the national RD system, Subprogram 1.2—Institutional Performance—RDI excellence funding projects, contract no.11PFE/30.12.2021, for financial support. The authors gratefully acknowledge to Nicolae Buzgar for valuable comments, and for access to ED-XRF spectrometer at Geology Department, UAIC. The use of the XRD, FTIR and SEM facilities at the National Geological Museum, Geological Institute of Romania, is kindly acknowledged. We extend our gratitude also to the anonymous reviewers for their time spent reading the first draft of our manuscript and for their valuable suggestions.

**Conflicts of Interest:** The authors declare no conflict of interest.

## References

1. Velde, B.; Meunier, A. *The Origin of Clay Minerals in Soils and Weathered Rocks*; Springer: Berlin, Germany, 2008; ISBN 978-3-540-75633-0.
2. Buggle, B.; Glaser, B.; Hambach, U.; Gerasimenko, N.; Marković, S. An evaluation of geochemical weathering indices in loess–paleosol studies. *Quat. Int.* **2011**, *240*, 12–21. [[CrossRef](#)]
3. Churchman, G.J.; Velde, B. *Soil Clays: Linking Geology, Biology, Agriculture, and the Environment*, 1st ed.; CRC Press: Boca Raton, FL, USA, 2019; Volume 277, ISBN 9780429154768.
4. Egli, M.; Mirabella, A. *The Origin and Formation of Clay Minerals in Alpine Soils*; American Geophysical Union: Washington, DC, USA, 2021. [[CrossRef](#)]
5. Perri, F. Chemical weathering of crystalline rocks in contrasting climatic conditions using geochemical proxies: An overview. *Palaeogeogr. Palaeoclimatol. Palaeoecol.* **2020**, *556*, 109873. [[CrossRef](#)]
6. Price, J.R.; Velbel, M.A. Chemical weathering indices applied to weathering profiles developed on heterogeneous felsic metamorphic parent rocks. *Chem. Geol.* **2003**, *202*, 397–416. [[CrossRef](#)]
7. Egli, M.; Mirabella, A.; Mancabelli, A.; Sartori, G. Weathering of soils in alpine areas as influenced by climate and parent material. *Clays Clay Miner.* **2004**, *52*, 287–303. [[CrossRef](#)]
8. Hamdan, J.; Burnham, C.P. The contribution of nutrients from parent material in three deeply weathering soils of Peninsular Malaysia. *Geoderma* **1996**, *74*, 219–233. [[CrossRef](#)]
9. Meunier, A.; Velde, B. *Illite: Origins, Evolution and Metamorphism*; Springer: Berlin, Germany, 2004; p. 286. ISBN 978-3-642-05806-6. [[CrossRef](#)]
10. Środoń, J. Nature of mixed-layer clays and mechanisms of their formation and alteration. *Annu. Rev. Earth Planet Sci.* **1999**, *27*, 19–53. [[CrossRef](#)]
11. Parker, A. An index of weathering for silicate rocks. *Geol. Mag.* **1970**, *107*, 501–504. [[CrossRef](#)]
12. Nesbitt, H.W.; Young, G.M. Formation and diagenesis of weathering profiles. *J. Geol.* **1989**, *97*, 129–147. [[CrossRef](#)]
13. Fedo, C.M.; Nesbitt, H.W.; Young, G.M. Unraveling the effects of potassium metasomatism in sedimentary rocks and paleosols, with implications for paleoweathering conditions and provenance. *Geology* **1995**, *23*, 921–924. [[CrossRef](#)]
14. Meunier, A.; Caner, L.; Hubert, F.; El Albani, A.; Pret, D. The weathering intensity scale (WIS): An alternative approach of the chemical index of alteration (CIA). *Am. J. Sci.* **2013**, *313*, 113–143. [[CrossRef](#)]
15. Kräutner, H.G. Syngenetic models for the pyrite and polymetallic sulphide ore province of the East Carpathian. In *Syngeneses and Epigenesis in the Formation of the Mineral Deposits*; Wauschkuhn, A., Kluth, C., Zimmermann, R.A., Eds.; Springer: Berlin, Germany, 1984; pp. 537–552.
16. Balintoni, I.; Balica, C. Carpathian peri-Gondwanan terranes in the East Carpathians (Romania): A testimony of an Ordovician, North-African orogeny. *Gondwana Res.* **2013**, *23*, 1053–1070. [[CrossRef](#)]
17. Stumbea, D.; Chicos, M.M.; Nica, V. Effects of waste deposit geometry on the mineralogical and geochemical composition of mine tailings. *J. Hazard. Mater.* **2019**, *368*, 496–505. [[CrossRef](#)] [[PubMed](#)]
18. Iftode, S.P. Mineralogy and Geochemistry of the Metamorphites and of the Sulphide Mineralization Associated from the Mănăila Area (Crystalline Mesozoic-Zone, Eastern Carpathians). Ph.D. Thesis, Alexandru Ioan Cuza University of Iasi, Iasi, Romania, 2012. Available online: [https://phdthesis.uaic.ro/\\_layouts/15/DocIdRedir.aspx?ID=PHDSERIES-1414501938-1146](https://phdthesis.uaic.ro/_layouts/15/DocIdRedir.aspx?ID=PHDSERIES-1414501938-1146) (accessed on 15 June 2022). (In Romanian).
19. Moldoveanu, S.P. Geochemical characteristics of rare earth elements and selected trace elements from the Mănăila ore deposit (Eastern Carpathians). *Carpath. J. Earth Environ. Sci.* **2012**, *7*, 193–198.
20. Chicos, M.M.; Damian, G.; Stumbea, D.; Buzgar, N.; Ungureanu, T.; Nica, V.; Iepure, G. Mineralogy and geochemistry of the tailings pond from Straja Valley (Suceava County, Romania). Factors affecting the mobility of the elements on the surface of the waste deposit. *Carpath. J. Earth Environ. Sci.* **2016**, *11*, 265–280.

21. Balintoni, I. The Crystalline-Mesozoic Zone of the East Carpathians. A review. In *Ore Deposits and Other Classic Localities in the Eastern Carpathians: From Metamorphics to Volcanics*; Iancu, O.G., Kovacs, M., Eds.; Acta Mineralogica-Petrographica. Field Guide Series; University of Szeged: Szeged, Hungary, 2010; Volume 19, pp. 13–21.
22. Google Earth. Available online: <https://earth.google.com/web/@47.85250831,23.25584237,210.87277493a,2445.5786484d,35y,0h,0t,0r> (accessed on 16 July 2021).
23. ICDD PDF-2 Database, database version 2.1302; sets 00–01–63 + 01–70–89 + 04–65–66 + 05–01; DDView program, version 4.13.3.6; JCPDS-ICDD—International Centre for Diffraction Data: Newtown Square, PA, USA, 2013.
24. Hoang-Minh, T.; Kasbohm, J.; Nguyen-Thanh, L.; Nga, P.T.; Lai, L.T.; Duong, N.T.; Thanh, N.D.; Thuyet, N.T.M.; Anh, D.D.; Pusch, R.; et al. Use of TEM-EDX for structural formula identification of clay minerals: A case study of Di Linh bentonite, Vietnam. *J. Appl. Cryst.* **2019**, *52*, 133–147. [[CrossRef](#)]
25. Sîrbu-Rădăşanu, D.S.; Buzgar, N. The geochemistry of major and selected trace elements in soil from northern area of Iasi city (Romania). *Carpath. J. Earth Environ. Sci.* **2013**, *8*, 63–74.
26. Iftode, S.P.; Huzum, R.; Sîrbu-Rădăşanu, D.S.; Buzgar, N.; Iancu, O.G.; Buzatu, A. Geochemical distribution of selected trace elements in the soil-plant system from Mănăila mining area, Romania. *An. Stiintifice De Univ. Al Cuza Din Iasi* **2015**, *61*, 21–31.
27. Okewale, I.A. Applicability of chemical indices to characterize weathering degrees in decomposed volcanic rocks. *Catena* **2020**, *189*, 10447. [[CrossRef](#)]
28. Nesbitt, H.W.; Young, G.M. Early Proterozoic climates and plate motions inferred from major element chemistry of lutites. *Nature* **1982**, *199*, 715–717. [[CrossRef](#)]
29. Munroe, J.S.; Norris, E.D.; Olson, P.M.; Ryan, P.C.; Tappa, M.J.; Beard, B.L. Quantifying the contribution of dust to alpine soils in the periglacial zone of the Uinta Mountains, Utah, USA. *Geoderma* **2020**, *378*, 114631. [[CrossRef](#)]
30. Musielok, L.; Drewnik, M.; Szymansky, W.; Stolarczyk, M.; Gus-Stolarczyk, M.; Skiba, M. Conditions favoring local podzolization in soils developed from flysch regolith—A case study from the Bieszczady Mountains in southeastern Poland. *Geoderma* **2021**, *381*, 114667. [[CrossRef](#)]
31. Skiba, M. Evolution of dioctahedral vermiculite in geological environments—An experimental approach. *Clays Clay Miner.* **2013**, *61*, 290–302. [[CrossRef](#)]
32. Moore, D.M.; Reynolds, R.C., Jr. *X-ray Diffraction and the Identification and Analysis of Clay Minerals*, 2nd ed.; Oxford University Press: Oxford, UK, 1997.
33. Bankole, O.; Albani, A.; Meunier, A.; Gauthier-Lafaye, F. Textural and paleo-fluid flow control on diagenesis in the paleoproterozoic franceville basin, south eastern, Gabon. *Precambrian Res.* **2015**, *268*, 115–134. [[CrossRef](#)]
34. Worden, R.H.; Griffiths, J.; Wooldridge, L.J.; Utley, J.E.P.; Lawan, A.Y.; Muhammed, D.D.; Simon, N.; Armitage, P.J. Chlorite in sandstones. *Earth-Sci. Rev.* **2020**, *204*, 103105. [[CrossRef](#)]
35. Szymanski, W.; Skiba, M.; Nikorych, V.A.; Kuligiewicz, A. Nature and formation of interlayer fillings in clay minerals in Albeluvisols from the Carpathian Foothills, Poland. *Geoderma* **2014**, *235*, 396–409. [[CrossRef](#)]
36. Hong, H.; Churchman, G.J.; Yin, K.; Li, R.; Li, Z. Randomly interstratified illite—Vermiculite from weathering of illite in red earth sediments in Xuancheng, southeastern China. *Geoderma* **2014**, *214*, 42–49. [[CrossRef](#)]
37. Müller, C.M.; Pejčić, B.; Esteban, L.; Piane, C.D.; Raven, M.; Mizaikoff, B. Infrared attenuated total reflectance spectroscopy: An innovative strategy for analyzing mineral components in energy relevant systems. *Sci. Rep.* **2014**, *4*, 6764. [[CrossRef](#)]
38. Goodman, A.; Sanguinito, S.; Tkach, M.; Natesakhawat, S.; Kutchko, B.; Fazio, J.; Cvetić, P. Investigating the role of water on CO<sub>2</sub>-Utica Shale interactions for carbon storage and shale gas extraction activities—Evidence for pore scale alterations. *Fuel* **2019**, *242*, 744–755. [[CrossRef](#)]
39. Zviagina, B.B.; Drits, V.A.; Dorzhieva, O.V. Distinguishing Features and Identification Criteria for K-Dioctahedral 1M Micas (Illite-Aluminoceladonite and Illite-Glaucanite-Celadonite Series) from Middle-Infrared Spectroscopy Data. *Minerals* **2020**, *10*, 153. [[CrossRef](#)]
40. Kowalska, J.B.; Skiba, M.; Maj-Szeliga, K.; Mazurek, R.; Zaleski, T. Does calcium carbonate influence clay mineral transformation in soils developed from slope deposits in Southern Poland? *J. Soils Sediments* **2021**, *21*, 257–280. [[CrossRef](#)]
41. González-Santamaría, D.E.; Justel, A.; Fernández, R.; Ruiz, A.I.; Stavropoulou, A.; Rodríguez-Blanco, J.D.; Cuevas, J. SEM-EDX study of bentonite alteration under the influence of cement alkaline solutions. *Appl. Clay Sci.* **2021**, *212*, 106223. [[CrossRef](#)]
42. Vaculikova, L.; Plevova, E. Identification of clay minerals and micas in sedimentary rocks. *Acta Geodyn. Geomater.* **2005**, *2*, 167–175.
43. Yang, M.; Ye, M.; Han, H.; Ren, G.; Han, L.; Zhang, Z. Near-infrared spectroscopic study of chlorite minerals. *J. Spectrosc.* **2018**, *695*, 8260. [[CrossRef](#)]
44. Warr, L.N. IMA—CNMNC approved mineral symbols. *Miner. Mag.* **2021**, *85*, 291–320. [[CrossRef](#)]
45. Bauer, A.; Velde, B. *Geochemistry at the Earth's Surface*; Springer: Berlin, Germany, 2016; Volume 327, ISBN 978-3-642-31359-2. [[CrossRef](#)]
46. Cox, R.; Lowe, D.R.; Cullers, R.L. The influence of de sediment recycling and basement composition on evolution of mudrocks chemistry in the southwestern United States. *Geochem. Cosmochim. Acta* **1995**, *59*, 2919–2940. [[CrossRef](#)]
47. Barré, P.; Montagnier, C.; Chenu, C.; Abbadie, L.; Velde, B. Clay minerals as a soil potassium reservoir: Observation and quantification through X-ray diffraction. *Plant Soil* **2008**, *302*, 213–220. [[CrossRef](#)]
48. Mei, H.; Jian, X.; Zhang, W.; Fu, H.; Zhang, S. Behavioral differences between weathering and pedogenesis in a subtropical humid granitic terrain: Implications for chemical weathering intensity evaluation. *Catena* **2021**, *203*, 105368. [[CrossRef](#)]

49. Penn, C.J.; Camberto, J.J. A critical review on soil chemical processes that control how soil pH affects phosphorus availability to plants. *Agriculture* **2019**, *9*, 120. [[CrossRef](#)]
50. Dzombak, R.D.; Sheldon, N.D. Weathering intensity and presence of vegetation are key control on soil phosphorus concentrations: Implication for past and future terrestrial ecosystems. *Soil Syst.* **2020**, *4*, 73. [[CrossRef](#)]
51. Skiba, M. Clay mineral formation during podzolization in an alpine environment of the Tatra Mountains, Poland. *Clays Clay Miner.* **2007**, *55*, 529–545. [[CrossRef](#)]
52. Hayes, N.R.; Buss, H.L.; Moore, J.W.; Kram, P.; Pancost, D. Controls on granitic weathering fronts in contrasting climates. *Chem. Geol.* **2020**, *535*, 130–132. [[CrossRef](#)]
53. Condie, K.C. Chemical composition and evolution of the upper continental crust: Contrasting results from surface samples and shales. *Chem. Geol.* **1993**, *104*, 1–37. [[CrossRef](#)]